

Granular packs under vertical tapping: structure evolution, grain motion, and dynamical heterogeneities

Massimo Pica Ciamarra* and Antonio Coniglio

Dipartimento di Scienze Fisiche, Università di Napoli 'Federico II' and INFM, Unità di Napoli, 80126 Napoli, Italia.

Mario Nicodemi

Department of Physics, University of Warwick, Coventry CV4 7AL, UK

The compaction dynamics of a granular media subject to a sequence of vertical taps made of fluid pulses is investigated via Molecular Dynamics simulations. Our study focuses on three different levels: macroscopic (volume fraction), mesoscopic (Voronoi volumes, force distributions) and microscopic (grain displacements). We show that the compaction process has many characteristics which are reminiscent of the slow dynamics of glass forming systems, as previously suggested. For instance the mean volume fraction slowly increases in time and approaches a stationary value following a stretched exponential law, and the associated compaction time diverges as the tapping intensity decreases. The study of microscopic quantities also put in evidence the existence of analogies with the dynamics of glass formers, as the existence of dynamical heterogeneities and spatially correlated motion of grains; however it also shows that there are important qualitative differences, as for instance in the role of the cage effect. Correlations between geometry and dynamics of the system at the grain level are put in evidence by comparing a particle Voronoi volume and its displacement in a single tap.

I. INTRODUCTION

When subject to vertical vibrations granular materials can produce a variety of distinct phenomena, depending both on the driving parameters and on the container properties. A great deal of interest has been recently raised by the process of compaction under successive vertical taps [1, 2, 3, 4, 5]. Experiments [1, 3, 4] show that the density of a column of grains submitted to vertical tapping increases slowly in time with a law well fitted by a stretched exponential [1] or logarithmic function [4], and that the characteristic compaction time grows abruptly as the driving intensity decreases. These observations have suggested an analogy with glass-forming systems, where the relaxation time diverges as the temperature is decreased; the analogy is corroborated by the fact that concepts like frustration and free volume, which are commonly used to explain the slow dynamics of supercooled liquids and other thermal systems, do also provide an insight in the physics of powder compaction [3, 6, 7].

However, contrary to supercooled liquids, granular materials are non-thermal systems as their typical energy scale, the energy required to rise a grain of its own diameter against gravity, is orders of magnitude larger than the thermal energy $k_B T$: each granular pack is in a mechanically stable state, which last as long as there is no external perturbation. Therefore even though the dynamics induced by a sequence of vertical taps becomes slower and slower as the tapping intensity decreases, important qualitative differences may exist between slow granular dynamics and glassy dynamics.

Here we investigate analogies and differences between granular dynamics and glassy dynamics by performing molecular dynamics (MD) simulations of a granular system subject to a sequence of vertical taps where, in order to explore a wide range of volume fractions, the system is tapped via flow pulses as in the experiment of Schröter *et. al.* [5]. We investigate the evolution of macroscopic quantities (volume fraction), mesoscopic quantities (Voronoi volumes, force distributions) and microscopic quantities (grain displacements), and we discuss how various static properties of a granular pack change during compaction [8]. We found several analogies between the compaction of granular media, and the slow dynamics of glass forming systems [9, 10, 11], as the divergence of the relaxation times, dynamical heterogeneities and spatially correlated motion; but we also show evidences of important qualitative differences, as in the role of the cage motion, which are put in evidence by the study of particle trajectories.

The paper is organized as follows. Sec. II presents the numerical model used. Then compaction dynamics, investigated via the study of the time dependence of the volume fraction, and of the diffusion coefficient at stationarity, is discussed in Sec. III. The evolution of structural properties of a compacting granular pack, the radial distribution function, the distribution of Voronoi volumes, and the distribution of interparticle forces, is presented in Sec. IV. Sec. V discusses the compaction dynamics at a grain level, showing the existence of dynamical heterogeneities and of spatially correlated motion of grains, and putting in evidence qualitative differences in the particle trajectories of compacting granular media and glass formers. Sec. V also presents a connection between geometrical (Voronoi volumes) and dynamical (particle displacements) properties of the system. Finally, a conclusion summarizes the main results and perspectives.

*picaciam@na.infn.it

II. NUMERICAL MODEL

We run Molecular Dynamics (MD) simulations of $N = 1600$ monodisperse spherical grains of diameter $d = 1\text{cm}$ and mass $m = 1\text{g}$. Grains, under gravity, are confined in a box with a square basis of length $L = 10\text{cm}$, with periodic boundary conditions in the horizontal directions. The bottom of the box is made of other immobile, randomly displaced, grains (to prevent crystallization). Simulations with 4 time more particles in a system with a square basis of length $2L$ give the same results, so we exclude the presence of finite size effect in our system.

Two grains in contact interact via a normal and a tangential force. The former is given by the spring-dashpot model, while the latter is implemented by keeping track of the elastic shear displacement throughout the lifetime of a contact [12]. The model is the one described in [13] with a restitution coefficient, $e = 0.8$. We use the linear model instead of the more realistic Hertzian model [14] as this latter is characterized by a coefficient of restitution which goes to zero as the relative velocity of the impacting particles decreases [12]. This feature makes computationally expensive the simulation of a granular system reaching a mechanically stable state.

The system is immersed in a fluid and, starting from a random configuration, it is subject to a dynamics made of a sequence of flow pulses where the fluid flows through the grains (see Fig.1), as in the experiment of Ref.[5]. In a single pulse the flow velocity, directed against gravity, is $V > 0$ for a time τ_0 ; then the fluid comes to rest. We model the fluid-grain interaction as in Ref.s [15, 16] via a viscous force proportional to the fluid grain relative velocity: $\mathbf{F}_{fg} = -A(\mathbf{v} - \mathbf{V})$ where \mathbf{v} is the grain and $\mathbf{V} = (0, 0, V)$ is the fluid velocity. The prefactor $A = \gamma(1 - \Phi_l)^{-3.65}$ is dependent on the local packing fraction, Φ_l , in a cube of side length $3d$ around the grain, and the constant is $\gamma = 1\text{Ns/cm}$ [16].

During each pulse, grains are fluidized and then come to rest under the effect of gravity g . The system is considered to be still when the kinetic energy per grains is below $10^{-5}mgd$. All measures below are recorded when the pack is at rest.

The dynamics of dry granular media subject to vertical vibrations is determined by two parameters, the amplitude and the frequency of vibrations. In the system we are investigating here there are also two parameters, the tap duration τ_0 and the fluid velocity V .

III. DYNAMICS

A. Volume fraction

When subject to a sequence of flow pulses a granular system compactifies (or expands) until it reaches a stationary state which depends on the driving parameters [5]. Fig. 2 shows the evolution of the volume fraction

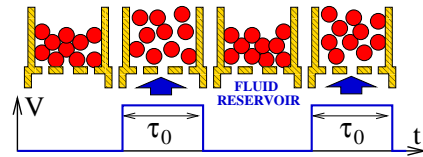


FIG. 1: (Color online) We study the compaction process of a granular media subject to flow pulses. During each pulse (tap), of duration τ_0 , fluid flows with velocity V through the granular media. Before applying a flow pulse we wait until the granular media comes to a rest.

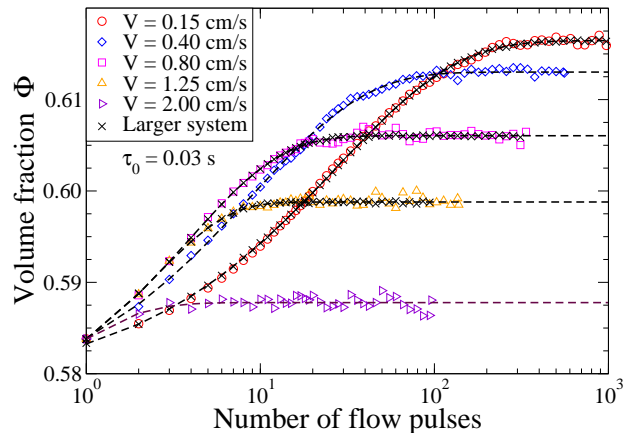


FIG. 2: (Color online) Temporal evolution of the mean volume fraction Φ for $\tau_0 = 0.03\text{s}$ and the reported values of fluid velocities V . The data obtained via simulations of a larger system (4 times more particles) evidence the absence of finite size effects. Dashed lines are fit to a stretched exponential law.

Φ (measured in the bulk of the system) with the number of flow pulses for systems subject to a tap dynamics with tap length $\tau_0 = 0.03\text{s}$ and various values of the fluid velocity V . Each curve is obtained by averaging over 32 independent realizations. Similar curves are obtained with different values of τ_0 .

The time evolution of the volume fraction is well described by a stretched exponential law,

$$\Phi(t) = \Phi_\infty - (\Phi_\infty - \Phi_0) \exp[-(t/\tau)^c], \quad (1)$$

with $c \simeq 1$. This is in agreement with experimental results of Philippe *et. al.* [1, 9, 17], which have investigated the relaxation dynamics of dry granular media subject to vertical taps in a system with a height to width ratio similar to ours. On the contrary Nowak *et. al.* [3, 4] have investigated a system with a larger height to width ratio, finding logarithmic compaction.

As in previous experiments of both vibrated [1, 3, 6, 18] and fluidized [5] granular systems, when the tapping intensity decreases the system compactifies more. This is clearly illustrated in Fig. 3, where we show the dependence of the volume fraction reached at stationarity on

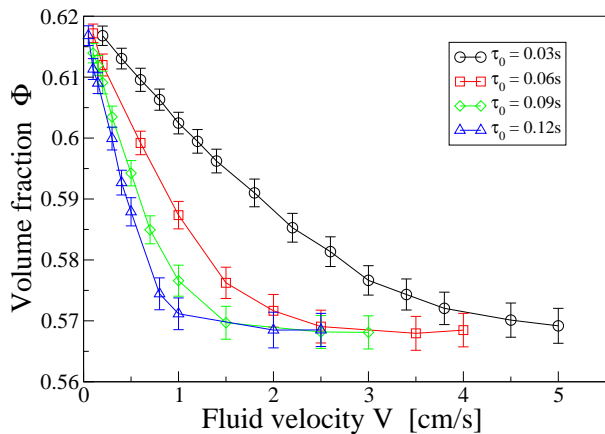


FIG. 3: (Color online) Dependence of the volume fraction reached at stationarity by a system subject to a sequence of flow pulses of length τ_0 on the fluid velocity V . Lines are a guide to the eye.

the fluid velocity V for various values of the tap length τ_0 . As one could have expected the final stationary state depends both on V and τ_0 . However it is possible to show numerically [19] that the final state can be characterized by one thermodynamical parameter, supporting the idea of a statistical mechanics description of granular media at rest [9, 20, 21, 22] originally proposed by S.F. Edwards [23].

B. Compaction time

The relaxation time τ which appears in Eq. 1 is a measure of the number of flow pulses required by the system to reach stationarity. The experiments of Ref. [5] have investigated a range of parameters V, τ_0 where the system reaches a stationary state after few flow pulses. On the contrary, the experiments of Bideau et. al. [1] have investigated a range of parameters where the compaction dynamics of the system is glassy like. They report a relaxation time following an Arrhenius behavior with the inverse maximum acceleration of the pack, $\tau \propto \exp(\Gamma^{-1})$. In the system under investigation here the relaxation time also evidences the existence of a glassy dynamics of the system, as it diverges with a power law with decreasing fluid velocity,

$$\tau \propto V^{-\beta} \quad (2)$$

with $\beta \simeq 1.17 \pm 0.04$, as shown in Fig. 4 (for data with tap length $\tau_0 = 0.03$ s). The same behavior is observed for different values of the tap length τ_0 .

C. Stationary dynamics

After having applied a long sequence of pulses up to reach the stationary state, we have computed the mean

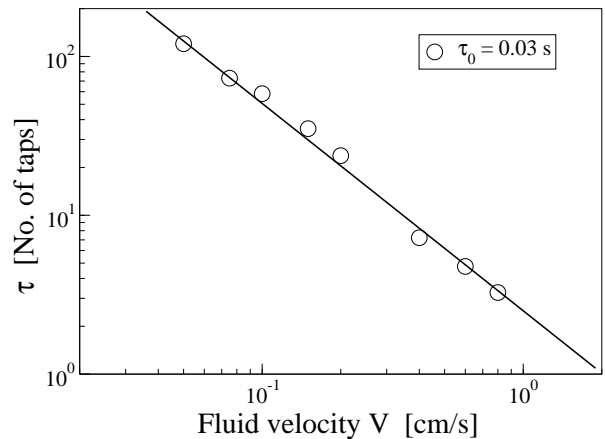


FIG. 4: The relaxation time τ increases with a power law (Eq. 2) as the fluid velocity decreases.

square displacement,

$$\langle r^2(t) \rangle = \frac{1}{N} \sum_i^N (\mathbf{r}_i(t + t_w) - \mathbf{r}_i(t_w))^2, \quad (3)$$

with $\mathbf{r}_i(t)$ position of grain i after t taps, and t_w waiting time which depends on the driving conditions ($t_w \simeq 3\tau$). From the mean square displacement, shown in Fig. 5, we have extracted the diffusion coefficient D ($\langle r^2(t) \rangle \propto Dt$) which decreases with the fluid velocity as a power law, $D \propto V^\beta$, with the same exponent observed for the dependence of the relaxation time on the fluid velocity (Fig. 5). This suggest the existence of relation $\tau \propto D^{-1}$ relating the compaction time and the diffusion coefficient at stationarity, which is illustrated in the inset of Fig. 5 (lower panel).

The mean square displacement evidences the absence of a subdiffusive regime in the slow dynamics of granular media subject to flow pulses, a signature of the cage effect in supercooled liquids. In Sec. V we will show that particles may be constrained in a cage, but that the escaping time is too small (few taps) in order to affect the mean square displacement.

IV. STRUCTURE EVOLUTION

A. Radial distribution function

The radial distribution function $g(r)$ is the probability distribution of finding the center of a particle in a given position at a distance r from a reference sphere. Since it contains information about long range interparticle correlations, it is a common tool in the characterization of packing structures. Here we study how the radial distribution functions, which we normalize as usual is such a way that $g(r) \rightarrow 1$ for $r \rightarrow \infty$, evolves during compaction.

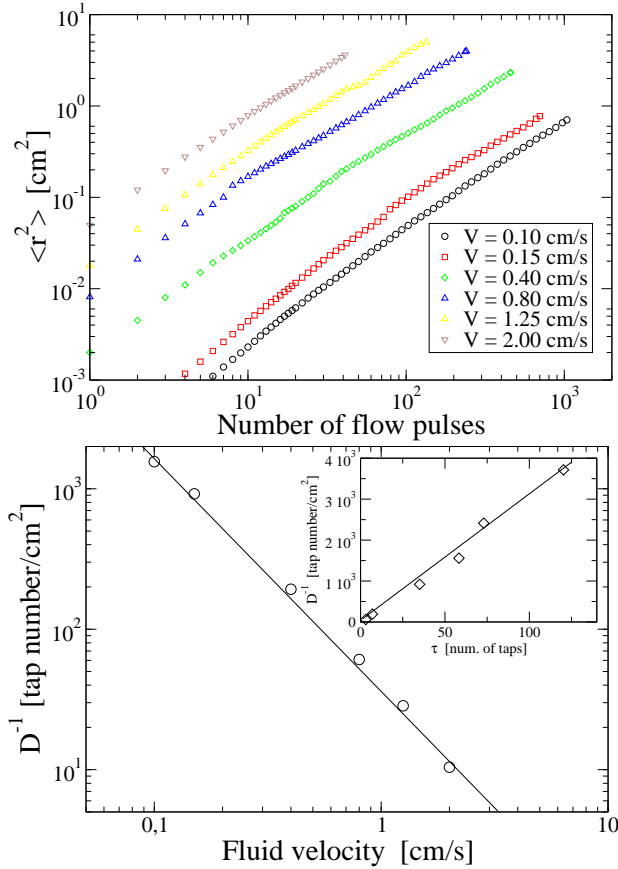


FIG. 5: (Color online) Left panel: mean square displacement (in the stationary state) for $\tau_0 = 0.03$ s and fluid velocities (from top to bottom) $V = 2.00, 1.25, 0.8, 0.40, 0.15$ and 0.10 cm/s. Right panel: the inverse diffusion coefficient (measured for those points in which the diffusion regime is attained) diverges as a power law, $D^{-1} = aV^{-\beta}$ as the fluid velocity V decreases. Inset: Stokes-Einstein relation between the compaction time and the diffusion coefficient at stationarity.

Fig. 6 (main frame) shows $g(r)$ at different times during compaction ($\tau_0 = 0.03$ s, $V = 0.2$ cm/s); similar results are found with different values of τ_0 and V . The first strong peak at $r = d = 1$ cm corresponds to the high probability of a having a neighbor in contact. This peak characterizes all dense systems of hard particles, as a consequence of their impenetrability. In a granular media at rest under gravity it is enhanced by the fact that, in order for the system to be stable, each grain must contact other grains. The following two maxima, as shown in the inset, appears at $r = \sqrt{3}d$ and $r = 2d$. Both of them increase with the volume fraction indicating an increasing organization of the packing (not necessarily related to the formation of ordered structures [25]). A similar dependence of the secondary peaks of the radial distribution function on the volume fraction has been observed experimentally by T. Aste *et al.* [25], which have investigated via x-ray tomography packs with different densities, and numerically by L.E. Silbert *et al.* [12].

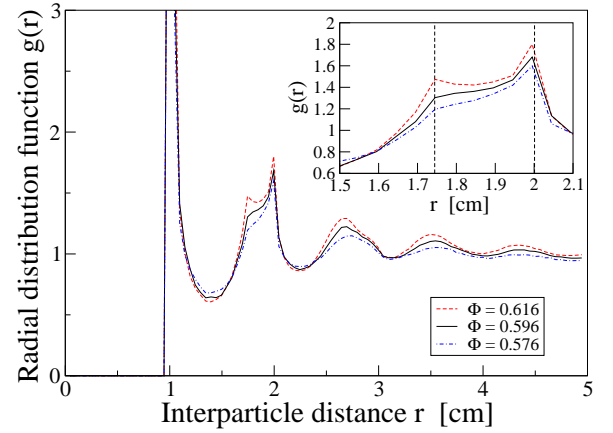


FIG. 6: (Color online) Radial distribution function for packing of volume fraction $\Phi = 0.576, 0.596$ and 0.616 . As the volume fraction increases we observe a small increment of the peaks at $\sqrt{3}d$ and $2d$, with $d = 1$ cm grain diameter.

B. Voronoï tessellation

In a granular pack of monodisperse spheres of volume fraction Φ the mean volume occupied by a particle is V_p/Φ , where V_p is the volume of a particle. When the system is in a disordered state there will be both particles occupying a larger volume, and particles occupying a smaller one. It is therefore instructive to investigate what is the probability that a given particle occupies a volume v , and how this probability changes during compaction.

To this end one has to operatively define what is the volume occupied by a particle: by using the Voronoï tessellation (as in [25]) we define the volume v_i occupied by particle i as the volume of the convex polyhedron which contains all points closer to particle i than to any other particle. Fig. 7.a shows the distribution $P(v)$ of the Voronoï volumes of a system tapped with $\tau_0 = 0.03$ s and $V = 0.2$ cm/s, after 1, 10, 100 and 300 taps. These are slightly asymmetric distributions with exponential tails (Fig. 7.a, inset). The asymmetry is a standard feature of the Voronoï distribution: for an ideal gas in one dimension, for instance, $P(v) \propto v\rho^2(1-\rho)^v$, where the Voronoï volume v of a given atom is half of the distance between its left and right nearest neighbors. As the system compactifies both the mean value $\langle v \rangle$ and the standard deviation σ_v of the distribution decrease. However the distribution retains its functional form: when $\sigma_v P(v)$ is plotted versus $(v - \langle v \rangle)/\sigma_v$ all of the different curves scale on the same master curve, as shown in Fig. 7.b. This scaling suggests the existence of a single geometrical structure of the system, only specified by its volume fraction, and tell us that there are no dramatic structural changes during compaction.

The same scaling of the distribution of Voronoï volumes has been observed by F.W. Starr *et al.* [26] in MD simulations of a glass-forming polymer melt, and is ver-

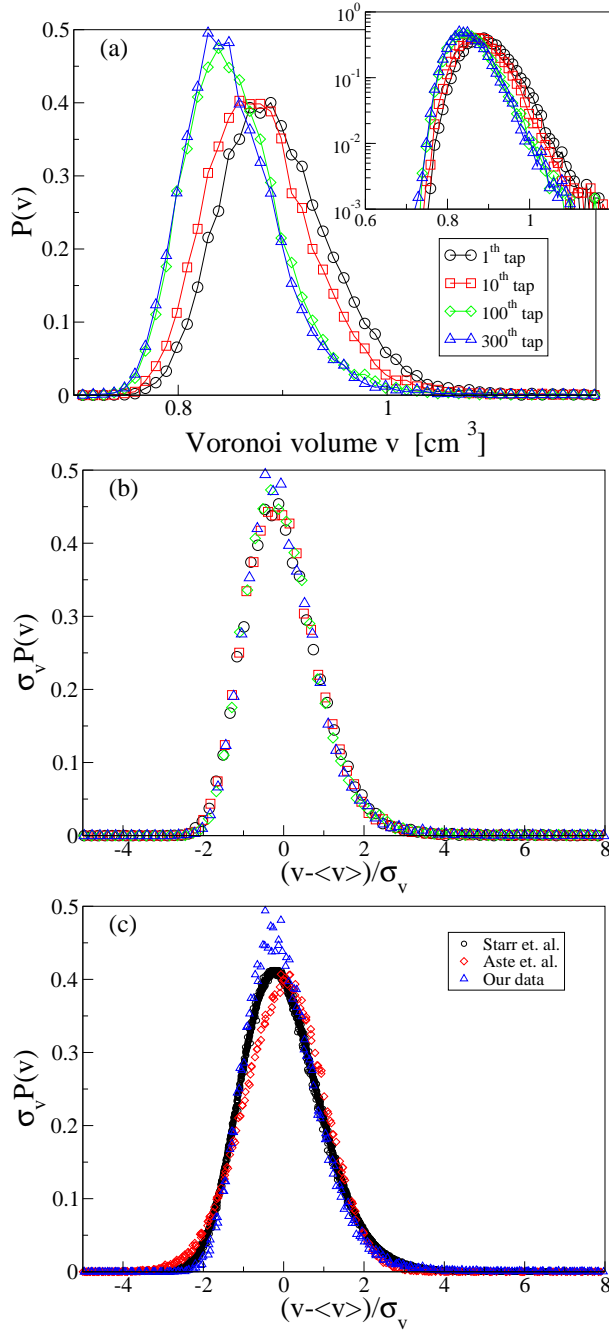


FIG. 7: (Color online) (a) Distribution of the Voronoi volumes in the sample after 1, 10, 100 and 300 taps. As the system compactifies the standard deviation σ_v and the mean value $\langle v \rangle$ of the distribution decrease. (b) Scaling of the distributions of the Voronoi volumes shown in Panel (a). Same symbols are used. (c) The same scaling has been found in MD simulations of a model of glass-forms by Starr *et al.* [26], and is verified by the experimental data of Aste *et al.* [25]. However data from different sources do not scale on the same master curve.

ified by the experimental data on granular packs of T. Aste *et al.* [25]. However the data from these different sources do not scale on the same master curve, as shown

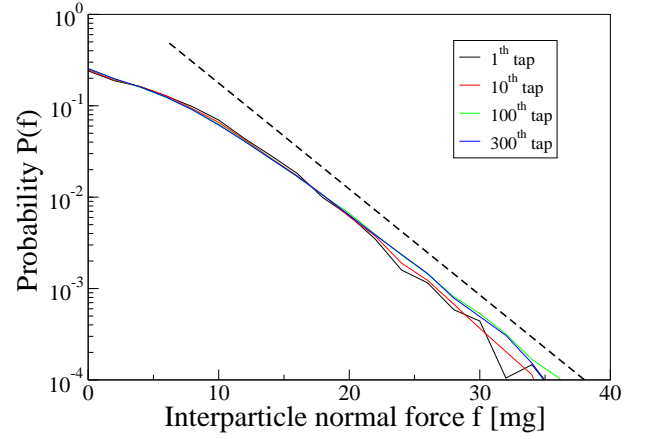


FIG. 8: (Color online) The distribution of interparticle normal forces decay exponentially at high forces, it appears to be insensitive on the packing fraction of the system.

in Fig. 7.c. The discrepancy which may be due to the fact that Ref. [26] investigates a thermal system, while Ref. [25] investigates a polydisperse system, needs further investigation.

C. Force distribution

Since the work of Mueth *et al.* [27] interparticle force distributions have become a standard tool for the characterization of granular packs. There are now experiments, numerical simulations and theories (see [28] and references therein) finding an exponential decay at high forces. This exponential decay is the signal of an heterogeneous structure of the system: while most of the interparticle normal forces have magnitude close to the mean value, there are also interparticle normal forces of much higher magnitude. Moreover, these high forces have been shown to be spatially related, giving rise to the well know force chains.

We have studied the evolution of the probability distribution of normal forces during compaction. In order to avoid the effect of gravity (due to the absence of vertical walls the mean vertical stress depends on the depth) we have computed the probability distribution of the normal forces between grains contacting in a point at a height z enclosed in a thin horizontal slice ($z > 8$ cm and $z < 10$ cm). Similar results are observed when selecting different horizontal slices of our system. Fig. 8 shows the force probability distribution after 1, 10, 100 and 300 taps (corresponding to volume fractions in the range 0.576 – 0.616). Since the distributions collapse on the same curve normal forces appears not to be affected by the density of the system (in the range we have investigated). We conclude that the force distribution is rather insensitive to the density of the granular pack, as also observed in Ref. [33] and in [34] (where it is show

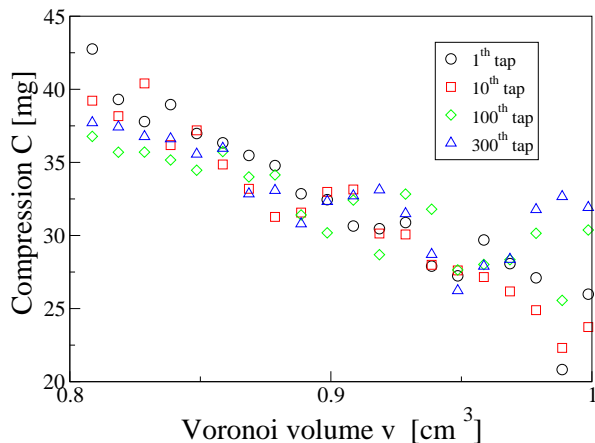


FIG. 9: (Color online) The compressional force C of a particle decreases with its Voronoi volume.

that forces do not couple with the density for thermal systems near the glass transition as well). It should be noted, however, that the use of the more realistic Herzian (instead of the linear) grain-grain interaction model (see Sec. II) may change the properties of the force distribution.

D. Force-Volume correlations

The relation between geometrical structure of the packing and interparticle forces has been investigated in a number of previous works (see [28] and reference therein). Here we report on a relation between the Voronoi volume associated to a particle and the forces acting on it. To this end we define the compressional force C_i acting on particle as:

$$C_i = \sum_{i \neq j} |\vec{f}_{ij}| \quad (4)$$

where $|\vec{f}_{ij}|$ is the normal force of interaction between particles i and j . C_i measures how much particle i is compressed as the pressure acting on it is C_i/S_i , where $S_i = 4\pi(d/2)^2$ is the particle surface. Fig. 9 shows that the compressional force decreases with the Voronoi volume.

A simple explanation of the decreasing of the compressional force with the Voronoi volume can be obtained via the following argument. Consider two contacting particles at a distance l . Their interparticle force decreases with l and particularly in our case, due to the computational model used, $f = k(d - l)$, where d is the diameter of a particle. On the other hand the Voronoi volume v of one of these particles increases with l . Assuming $v \propto l^\alpha$, one obtains $f \propto (d - v^{1/\alpha})$, i.e. a decrease of the compressional force with the Voronoi volume. The data of Fig. 9 are consistent with $\alpha = 3$, as expected for dimensional

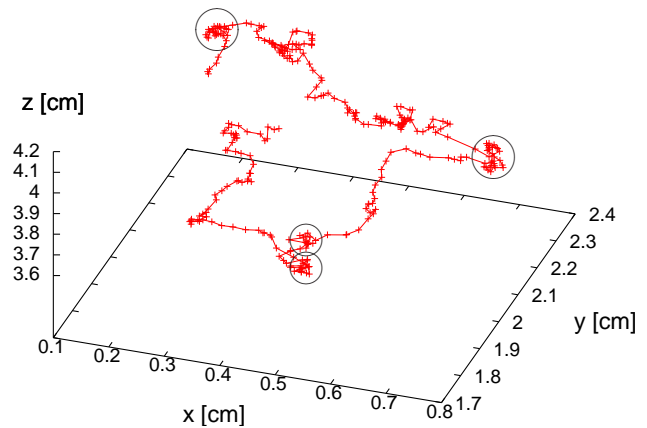


FIG. 10: (Color online) Typical trajectory of a particle during compaction, followed for 300 taps during compaction ($V = 0.2$ cm/s, $\tau_0 = 0.03$ s). Circles illustrate that sometimes a particle is confined in cages formed by its neighbors.

reasons. However a reliable estimate of α is difficult to obtain as Voronoi volumes vary in a small range.

V. GRAIN MOTION

In this section we investigate how a granular pack moves during a single tap. We consider a system subject to a tap dynamics with $\tau_0 = 0.03$ s and $V = 0.2$ cm/s, and compare the state reached after the application of n taps, with the state reached after the application of one more tap (with $n = 1, 10, 100, 300$).

Particularly we investigate the distribution of particle displacements, the heterogeneity of particle motion, and the correlation between a particle displacement and both its Voronoi volume and the compressive force acting on it.

A. Particle trajectory and cage motion

Fig. 10 shows a typical trajectory of a particle during compaction. As observed in colloidal systems the trajectory is characterized by period of time in which the particle is confined in cages formed by its neighbors. Cage motion has also been observed before in experiment of granular materials subject to continuous vibrations [29] and to shear [30, 31, 32].

The typical linear size of the cage is roughly $0.05d$, where $d = 1$ cm is the diameter of the particles. A similar ratio between cage size and particle size has been observed in [36]. However there is an important qualitative difference between the motion of a particle in colloidal suspension and other glass forming systems, and that observed in our system. In glass forming systems a particle spend most of its time rattling inside a cage,

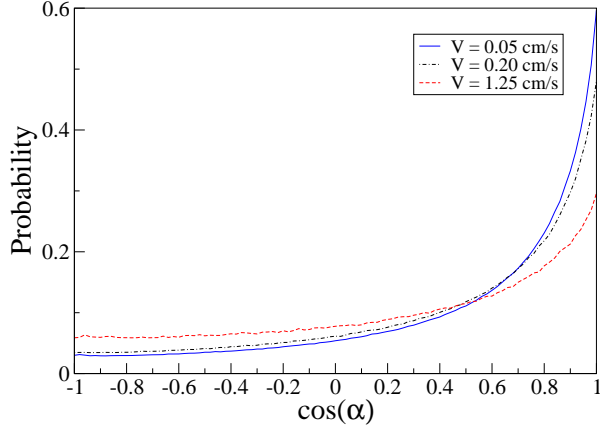


FIG. 11: (Color online) Probability distribution of $\cos(\alpha)$, where α is the angle formed by the displacements $\vec{\Delta}$ of a particle in two subsequent taps. The distribution evidences that particles usually travel along straight lines, and that this tendency increases as the driving intensity decreases.

from which it escape via infrequent cage-breaking rearrangements. Here we observe the opposite behavior: particles usually diffuse, and sometimes they get trapped in a cage. This unusual property of the trajectory is put in evidence by the study of the distribution of the angle α formed by the displacement $\vec{\Delta}_n$ of a particle during tap n , and the displacement $\vec{\Delta}_{n+1}$ of the same particle during the following tap. Figure. 11 shows the distribution of

$$\cos(\alpha) = \frac{\vec{\Delta}_n \cdot \vec{\Delta}_{n+1}}{|\vec{\Delta}_n| |\vec{\Delta}_{n+1}|}, \quad (5)$$

which is strongly peaked near 1. This is a clear indication that particles usually move along straight lines (as also confirmed by Fig. 10), and that cage motion is negligible: for a particle rattling in a cage two consecutive displacements have opposite direction, and $\cos(\alpha) \simeq -1$.

The absence of cage motion is due to the driving mechanism. During a tap the system expands, cages break, and it is easier for the grains to move one with respect to the other.

B. Particle displacements

Here we investigate the evolution of the distribution of particle displacements during a single tap. After the application of a flow pulse to our system (and the following relaxation) a particle i , initially located in \vec{r}_i , will be in a new position position $\vec{r}_i + \vec{\Delta}_i$, where $\vec{\Delta}_i$ denotes its displacement. We examine below the probability that a particle makes a given displacement $\vec{\Delta}$. Due to presence of gravity, which breaks the up-down symmetry of the system, it is convenient to separate the vertical component of the displacement, Δz_i , from the horizontal ones,

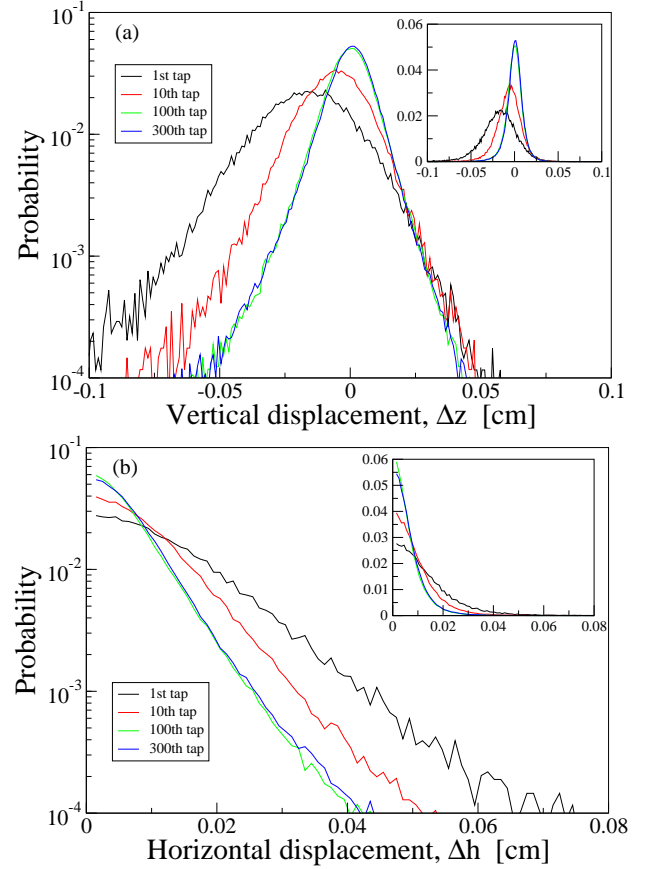


FIG. 12: (Color online) Probability distribution of vertical (Δz , upper panel) and horizontal (Δh , lower panel) displacements of a grain during the 1st, 10th, 100th and 300th tap in semi-logarithmic (main panels) and linear (insets) scale.

Δx_i and Δy_i . As Δx_i and Δy_i have the same, even distribution, we have studied the evolution of the distribution of $\Delta h = |\Delta x|$ ($|\Delta y|$). In order to follow the dynamics of the system, in Fig. 12 we have plotted the probability distribution of Δz , $P_z(\Delta z)$, (upper panel) and of Δh , $P_h(\Delta h)$, (lower panel) during tap number 1, 10, 100 and 300.

During the compaction process displacements with $\Delta z < 0$ are more probable than those with $\Delta z > 0$. Therefore, as shown in Fig. 12 (upper panel), $P_z(\Delta z)$ is asymmetrical. The asymmetry of the distribution decreases as the system compactifies and after 300 taps, when stationarity is almost attained, $P_z(\Delta z)$ appears to be nearly symmetric. Accordingly the value of Δz where $P_z(\Delta z)$ has its maximum increases, starting from a negative value, until it reaches zero. Also, it is apparent that as the system compactifies the variance of the distribution decreases. The probability of a large vertical displacement to occur is smaller in a dense rather than in a fluffy system. This is also true for the probability of large horizontal displacements, as shown in Fig. 12 (lower panel).

An important feature of the probability of both vertical and horizontal displacements is the nearly exponential decay at large displacements. This is an indication of the fact that, while during a tap most of the particles are subject to small displacements, very few of them may move much more. We conclude that the system is characterized by an heterogeneous dynamics. This is a well know property of thermal systems, like liquids or colloids (see [37] for a review), which appears upon cooling the system near the glass transition. For instance, in colloidal systems the exponential tail of the particle displacement distribution has been experimentally observed by Weeks *et. al.* [36].

The probability distribution function of particles displacements can be further analyzed via the study of the excess-kurtosis

$$\alpha_2^{(i)} = \frac{\langle (\Delta_i - \langle \Delta_i \rangle)^2 \rangle^2}{3 \langle (\Delta_i - \langle \Delta_i \rangle)^4 \rangle} - 1, \quad i = h, z, \quad (6)$$

a comparison between the second and the fourth central moment of the distribution, which is zero for a gaussian distribution. We have first considered the excess-kurtosis as obtained from the probability of particle displacements in a single tap: α_2^h and α_2^z fluctuate from tap to tap, and their mean values are $\alpha_2^h = 2.8 \pm 0.1$, $\alpha_2^z = 4.3 \pm 0.2$. This positive values indicate that the probability distribution of particle displacements is more peaked with respect to a gaussian distribution. Then, we have considered the excess-kurtosis of the probability distribution of the horizontal and vertical components of $\vec{r}_i(n) - \vec{r}_i(n_0)$, the total displacement of a grain after tap n_0 , where $n_0 = 100$ correspond to the compaction time. As expected from the central limit theorem at long times this excess-kurtosis is zero: Fig. 13 shows, interestingly, that in our system the excess kurtosis approach zero with a monotonic decay. This is in sharp contrast with the observations made in glass forming system, as in Ref. [36], where a peak is observed at the α relaxation time, i.e., when cage rearrangements occur. Therefore Fig. 13 confirms the marginal role played by cage motion in our system.

Our results put in evidence a very smooth behavior of the particles displacement distribution. Particularly we have not observed any ‘rare event’ (displacement of the order of 0.4 particle diameters), recently observed by Ribière and coworkers [35] in the study of a granular system undergoing compaction. This is probably due to the different driving mechanism of the systems. In shaken system, in fact, grains move one with respect to the other mainly when the pack settle downs and a shock wave propagates upwards; in our system, on the contrary, there is not a shock wave propagating as grains settle down slowly, and relative grain motion occurs during the tap.

C. Spatial heterogeneous dynamics

In supercooled liquids and dense colloidal systems the dynamics is heterogeneous as there are both slow and

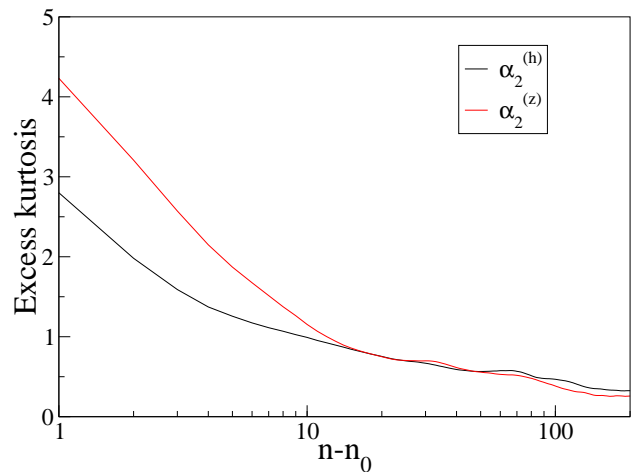


FIG. 13: Time variation of the excess kurtosis of the probability distributions of the total horizontal (α_2^h) and vertical (α_2^z) displacements of a grain since tap $n_0 = 100$. The monotonic decay evidences the marginal role played by cage motion in our system.

fast particles. Moreover, fast particles are known to be spatially correlated as they appear to form clusters [36, 37, 38]. Here we show that the exact same tendency characterizes a granular system subject to vertical taps, as suggested in Ref.s [39, 40].

In order to characterize the spatially heterogeneous dynamics [38, 41, 42] one usually resorts to a four-point time-dependent density correlation function and to its fluctuations (susceptibility). This latter measures the correlated motion between pairs of particles. As this motion is decorrelated on short and long times, the susceptibility shows a well defined maximum at a given time. Unfortunately we cannot follow this line here as many averages are needed in order to get clear data on the fluctuations, and our simulations are computationally too expensive. Moreover during compaction the system is not in a stationary state. In order to measure the degree of spatially heterogeneous dynamics we have therefore used a different method, based on the comparison between our system and a random one, as discussed below.

We apply k flow pulses ($k = 1, 10, 100, 300$) to our system (who reaches volume fraction 0.576, 0.596, 0.612, 0.616) and we determine the n_p particle having experienced the largest displacement during the last tap. Here $n_p = pN$, where $N = 1600$ is the total number of particles, $p = 1\%, 2\%, 5\%$ and 10% . When these fast particles are drawn, as in Fig. 14, it is apparent that they form clusters, a clear evidence of the spatially heterogeneous dynamics. We have quantified the degree of heterogeneity of the system as follows. After every tap we have determined the n_p faster particles of the system, and determined the number s_p of couples of these particles made of neighboring particles (we consider two particles to be neighbor if

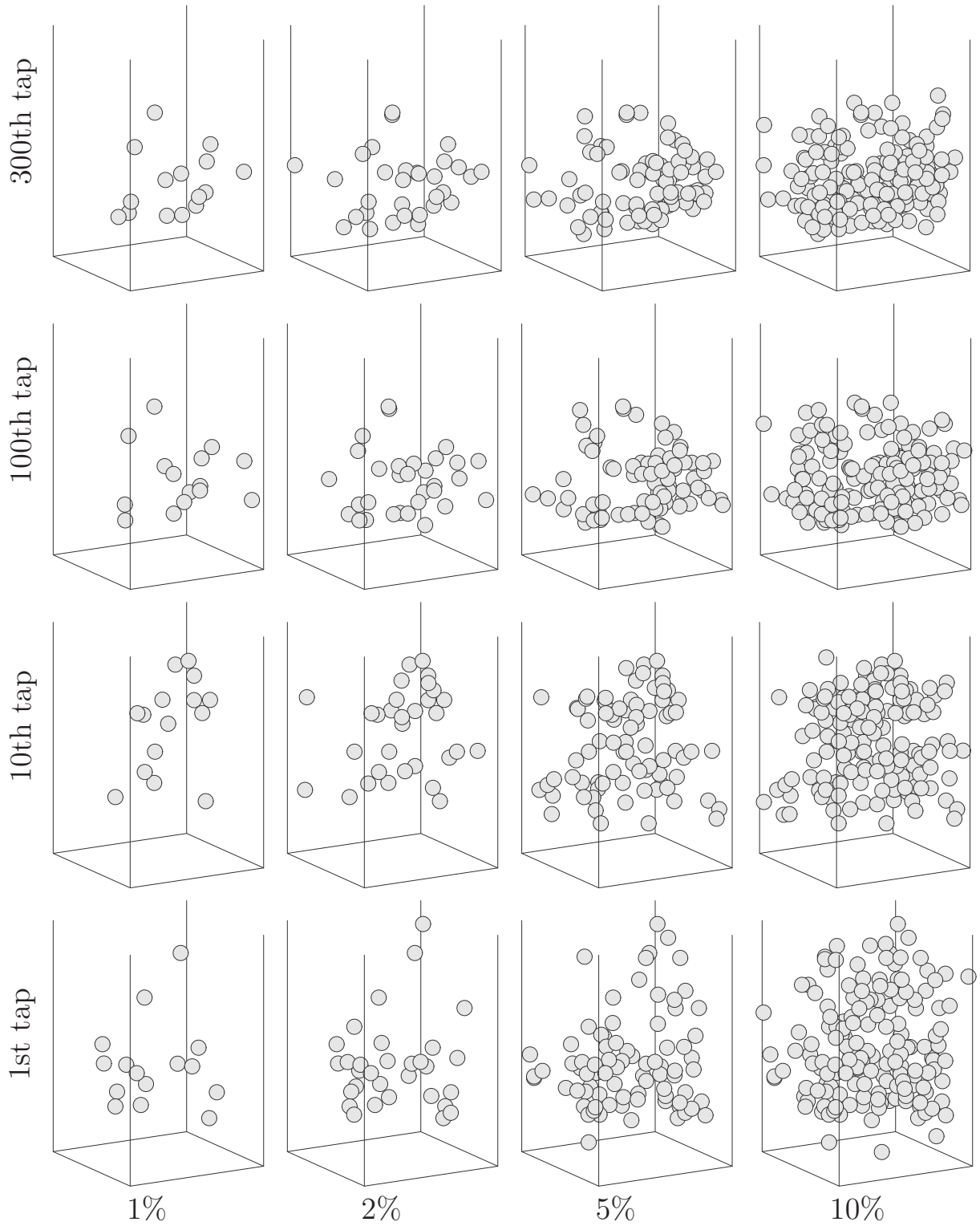


FIG. 14: Granular compaction is characterized by a spatially heterogeneous dynamics. After the k th tap ($k = 1, 10, 100, 300$, and volume fraction $\Phi = 0.576, 0.596, 0.612, 0.616$) we plot the position of the n_p particles which have experienced the largest displacement during the last tap, with $n_p = pN$ and $p = 1\%, 2\%, 5\%$ and 10% .

the distance between their center is smaller than 1.2 particle diameters). Then we have computed the same

quantity s_p^{random} in the case of n_p randomly selected particles of the system. A measure of the degree of

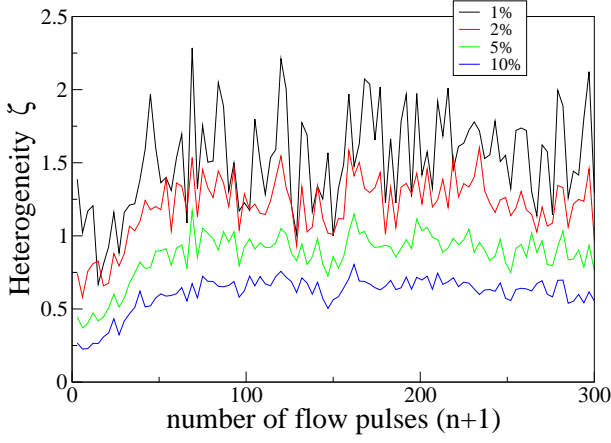


FIG. 15: (Color online) Granular compaction is characterized by a spatially heterogeneous dynamics. This is quantified by the parameter ξ_p (see Eq. 7) which is plotted here as a function of the number of taps for $p = 1\%, 2\%, 5\%$ and 10% (from top to bottom).

spatial heterogeneous dynamics is given by

$$\xi_p = \frac{s_p - s_p^{\text{random}}}{s_p^{\text{random}}}. \quad (7)$$

Clearly $\xi_p \simeq 0$ for an homogeneous systems, $\xi_p > 0$ if faster particles form clusters, while $\xi_p < 0$ if faster particles tend to be apart. Fig. 15 shows the evolution of ξ_p with the number of taps. In all cases $\xi_p > 0$, signaling the presence of an heterogeneous dynamics. When the system approaches the steady state, and compaction stops, ξ_p fluctuates around a plateau which varies with p between 0.5 and 1.5. These are very high values, indicating a high degree of spatial heterogeneity of the system.

D. Volume-Displacement correlation

It is well known than many equilibrium and transport properties of dense fluids depend on the space available for molecular motion. For instance the well known *free volume* theory developed by Choen and Turnbull [43] to explain the divergence (with a Vogel-Tamman-Fulcher law) of the relaxation time of many glass formers as the temperature is decreased, is based on the idea that the space available for molecular motion decreases with the temperature. It is therefore interesting to check for correlations between the displacement of a particle and its free volume in our granular system. There are many possible way to define the free volume of a particle. Here we approximate, for simplicity sake, we consider the free volume of particle i to be $V_i^F = v_i - V_0$, where v_i is the Voronoï volume of the particle (see Sec. IV B) before the application of a tap, and $V_0 = 4/3\pi(D/2)^3$ its volume. The displacement Δ_i of particle i ($\Delta_i =$

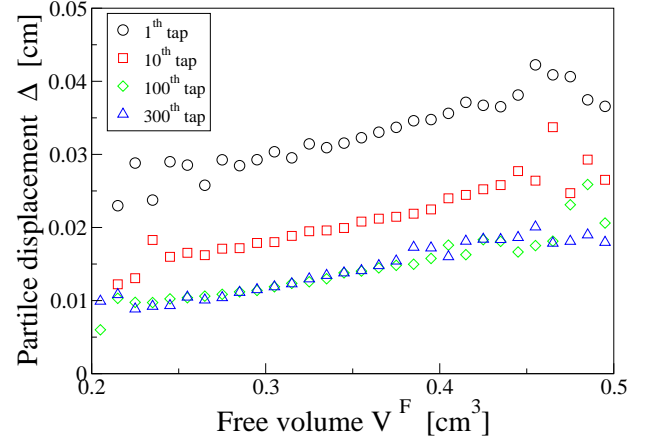


FIG. 16: (Color online) The mean displacement Δ of particle during a single tap increases with its Voronoï volume v . The displacements are measured during tap 1, 10, 100 and 300, when the volume fraction of the system is 0.576, 0.596, 0.612, 0.616.

$(\Delta_x^2 + \Delta_y^2 + \Delta_z^2)^{1/2}$) is the distance between the position of the particle before and after the application of the tap.

A possible connection between V_i^F and Δ_i is suggested by the similarity between the the probability distribution functions of Voronoï volumes (see Fig. 7.a), and that of particles displacements (Fig. 12). Both of them have an exponential tail at high values. Moreover they evolve in a qualitatively similar way (the variance and the mean value decrease) as the system compactifies.

In order to test this possible correlation we have computed during the n th tap ($n = 1, 10, 100, 300$) ($\tau_0 = 0.03$ s, $V = 0.2$ cm/s) the mean value of the displacement Δ of all the particles with free volume V^F . The dependence of Δ on V^F is shown in Fig. 16. This figure puts in evidence the existence of an almost linear correlation between Voronoï volumes and particle displacements, with $\partial\Delta/\partial v \simeq 0.01/0.2 = 0.05$ cm⁻²: the larger the Voronoï volume of a particle, the bigger its displacement.

E. Force-Displacement correlation

In the previous paragraph we have shown that there is a correlation between the displacement Δ of a particle during a single tap, and its free volume. Fig. 17 investigates the correlation between displacement and compression C (see Eq. 4) of a particle. The figure puts in evidence that for small values of the compressional force there is a decreasing linear relation between displacement and compression of a particle, while for higher value of the compressional force the two becomes uncorrelated.

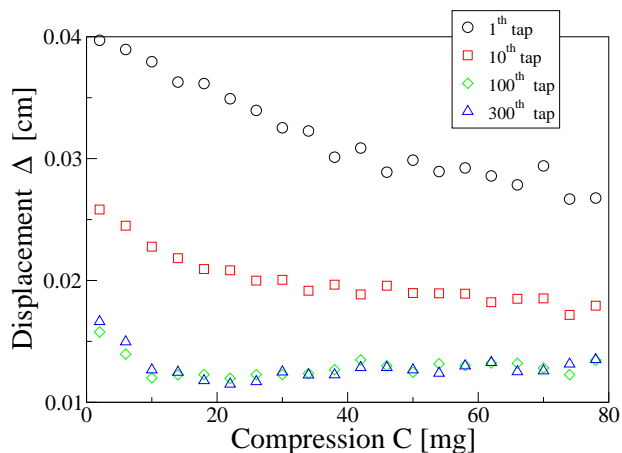


FIG. 17: (Color online) The mean displacement Δ of a grain as a function of its compressional force. When the packing is loose grains with higher compressional forces move less. As the granular pack compactifies the displacement of a particle appears not to depend on its compression.

VI. CONCLUSIONS

We have reported results of a numerical simulations of a packing of monosize spheres submitted to vertical taps made of flow pulses as in the experiment of Ref. [5]. Our results relative to the dynamics of the systems confirms earlier experimental observation: as the intensity of vibration decreases both the value of the volume fraction reached at stationary and the compaction time increases [1, 3, 5, 6, 18]. The increase of the compaction time with the decreasing of the vibration intensity is dramatic as this appears to diverge with a power law when the fluid velocity goes to zero.

The analysis of the evolution of several structural quantities during compaction has revealed that this is not accompanied by any particular geometrical modification. The radial distribution function and the Voronoï volume distribution, for instance, smoothly change as the den-

sity of the granular system increases. In particular the collapse of the Voronoï volume distributions (sec. IV B) evidences the presence of a single underlying geometrical structure in the system. Also, the probability distribution function of normal forces between grains do not change during compaction.

The analysis of the dynamics of compaction has revealed that this is characterized by dynamical heterogeneities. The probability that, during a tap, a particle makes a given displacement decreases exponentially with its size, resembling observations made in dense colloidal systems [36]. Similarly we have observed that, during a tap, faster particle tend to form cluster, as observed both in colloidal [36] and in glass-forming [37, 38, 41] systems. There is, however, a marked difference between a typical trajectory of a granular particle during compaction, and a typical trajectory of a particle in supercooled liquids. Precisely, in supercooled liquids a particle spend most of time in cages formed by its neighbors, and occasionally makes large displacement escaping from the cage. In our system, instead, particles usually diffuse, and sometimes are trapped in a cage. This different behaviour is due to the particular driving of our system as in our system, when the the flow in on the system expands and the grains are able to escape from their cages.

As the slowdown of the dynamics is related to the space available for particle motion, we have studied the correlation between the displacement of particle during a tap and its Voronoï volume, which is a rough estimate of its free volume. This analysis has shown that particles with larger Voronoï volumes are those who make larger displacements during a tap.

Acknowledgements

We thank A. de Candia, A. Fierro, M. Schröter and M. Tariza for helpful discussions, F.W. Starr and T. Aste for sharing their data. Work supported by EU Network Number MRTN-CT-2003-504712, MIUR-PRIN 2004, MIUR-FIRB 2001, CRdC-AMRA, INFM-PCI.

-
- [1] P. Philippe and D. Bideau, *Europhys. Lett.* **60**, 677 (2002).
 - [2] A.D. Rosato and D. Yacoub, *Powder Tech.* **109**, 255 (2000).
 - [3] E.R. Nowak, J.B. Knight, E. Ben-Naim, H.M. Jaeger and S.R. Nagel, *Phys. Rev. E* **57**, 1971 (1998).
 - [4] J.B. Knight, C.G. Fandrich, C.N. Lau, H.M. Jaeger and S.R. Nagel, *Phys. Rev. E*, **51**, 3957 (1995).
 - [5] M. Schröter, D.I. Goldman, H.L. Swinney, *Phys. Rev. E* **71**, 030301(R) (2005).
 - [6] E. Ben-Naim *et al.*, *Physica D* **123**, 380 (1998).
 - [7] M. Nicodemi, A. Coniglio and H. J. Herrmann, *Phys. Rev. E*, **55**, 3962 (1997).
 - [8] P. Richard, P. Philippe, F. Barbe, S. Bourles, X. Thibault and D. Bideau, *Phys. Rev. E* **68**, 020301(R) (2003).
 - [9] A. Coniglio, A. Fierro, H.J. Herrmann and M. Nicodemi (eds), *Unifying Concepts in Granular Media and Glasses* (Elsevier, Amsterdam, 2004).
 - [10] A.J. Liu and S.R. Nagel, *Nature* **396**, 21 (1998).
 - [11] A. Fierro, M. Nicodemi, M. Tarzia, A. de Candia, and A. Coniglio, *Phys. Rev. E* **71**, 061305 (2005); M. Tarzia, A. de Candia, A. Fierro, M. Nicodemi, and A. Coniglio, *Europhys. Lett.* **66**, 531 (2004).
 - [12] L.E. Silbert, D. Ertas, G.S. Grest, T.C. Halsey, D. Levine and S.J. Plimpton, *Phys. Rev. E* **64**, 051302 (2001).
 - [13] We use the model 'L3' described in detail in Ref. [12].
 - [14] L.D. Landau and E.M. Lifshitz E. M., *Theory of Elasticity* (Oxford University Press, Oxford, 1965).

- [15] P. Sánchez, M.R. Swift, and P.J. King, Phys. Rev. Lett. **93**, 184302 (2004).
- [16] C. Crowe, M. Sommerfeld and Y. Tsuji, *Multiphase flows with droplets and particles* (CRC Press, Boca Raton, FL, 1998).
- [17] P. Philippe and D. Bideau, Phys. Rev. E **63**, 051304 (2001).
- [18] E.R. Nowak *et. al.*, Powder Tech. **94**, 79 (1997).
- [19] M. Pica Ciamarra, A. Coniglio and M. Nicodemi, Phys. Rev. Lett. **97**, 158001 (2006).
- [20] A. Fierro, M. Nicodemi, and A. Coniglio, Phys. Rev. E **66**, 061301 (2002).
- [21] H.A Makse and J. Kurchan, Nature **415**, 614 (2002).
- [22] G. D’Anna, P. Mayor, A. Barrat, V. Loreto and F. Nori, Nature **424** 909 (2003); A. Barrat, J. Kurchan, V. Loreto and M. Sellitto, Phys. Rev. Lett. **85**, 5034 (2000); Phys. Rev. E **63** 051301 (2001); M. Sellitto, Phys. Rev. E **66**, 042101 (2002); A. Barrat, V. Colizza, and V. Loreto, Phys. Rev. E **66**, 011310 (2002); V. Colizza, A. Barrat, and V. Loreto, Phys. Rev. E **65**, 050301(R) (2002).
- [23] S.F. Edwards and R.B.S. Oaskeshott, Physica A **157**, 1090 (1989); A. Metha and S.F. Edwards, Physica A, **157**, 1091 (1989); S.F. Edwards and C. C. Mounfield, Physica A, **210**, 290 (1994).
- [24] P. Richard *et. al.*, Nature Materials **4**, 121 (2005).
- [25] T. Aste, M. Saadatfar and T.J. Senden, Phys. Rev. E **71**, 061302 (2005); T. Aste, J. Phys.: Condens. Matter **17**, S2361 (2005); T. Aste, Phys. Rev. Lett. **96**, 018002 (2006).
- [26] F.W. Starr, S. Sastry, J.F. Douglas and S.C. Glotzer, Phys. Rev. Lett. **89**, 125501 (2002).
- [27] D.M. Mueth, H. M. Jaeger, and S.R. Nagel, Phys. Rev. E **57**, 3164 (1998).
- [28] J.H. Snoeijer, M. van Hecke, E. Somfai and W. van Saarloos, Phys. Rev. E **70**, 011301 (2004).
- [29] S. Warr and J.P. Hansen, Europhys. Lett. **36**, 589 (1996).
- [30] O. Pouliquen, M. Belzons, and M. Nicolas, Phys. Rev. Lett. **91**, 014301 (2003) .
- [31] G. Marty and O. Dauchot, Phys. Rev. Lett. **94**, 015701 (2005)
- [32] O. Dauchot, G. Marty and G. Biroli, Phys. Rev. Lett. **95**, 265701 (2005)
- [33] D.L. Blair, N.W. Mueggenburg, A. H. Marshall, H. M. Jaeger and S.R. Nagel, Phys. Rev. E **63**, 041304 (2001).
- [34] C.S. O’Hern, S.A. Langer, A.J. Liu and S.R. Nagel, Phys. Rev. Lett. **86**, 111 (2001).
- [35] P. Ribi  re *et. al.*, Phys. Rev. Lett. **95**, 268001 (2005).
- [36] E.R. Weeks *et. al.*, Science **287**, 627 (2000).
- [37] M.D. Ediger, Annu. Rev. Phys. Chem. **51**, 99 (2000).
- [38] S.C. Glotzer, J. Non-Cryst. Solids **274**, 342 (2000).
- [39] J. Arenzon, Y. Levin and M. Sellitto, Physica A **325**, 371 (2003).
- [40] A. Lef  vre, L. Berthier and R. Stinchcombe, Phys. Rev. E **72**, 010301(R) (2005).
- [41] N. La  vi   and S.C. Glotzer, J. Chem. Phys. B **108**, 19623 (2004).
- [42] W. Kob, C. Donati, S.J. Plimpton, P.H. Poole and S.C. Glotzer, Phys. Rev. Lett. **79**, 2827 (1997).
- [43] M.H. Choen and D.J. Turnbull, J. Chem. Phys. **31**, 1164 (1959).